Bull. Mater. Sci., Vol. 34, No. 7, December 2011, pp. 1511–1516. © Indian Academy of Sciences.

# Effects of MO (M = Mg, Ca, Ba) on crystallization and flexural strength of semi-transparent lithium disilicate glass–ceramics

**ZHIWEI LUO, JUNLIN ZHOU, JING LI, CHANGJIAN ZHANG and ANXIAN LU***
School of Materials Science and Engineering, Central South University, Changsha 410083, P.R. China

MS received 13 May 2010; revised 14 September 2010

**Abstract. In this study, semitransparent lithium disilicate glass–ceramics in the $Li_2O$–$K_2O$–$Al_2O_3$–$Y_2O_3$–$La_2O_3$–$SiO_2$ system was investigated by incorporation of $P_2O_5$ as nucleation agent and alkaline earth oxides as additive. The influence of alkaline earth oxides on the structure of glasses network, crystalline phases, microstructure and mechanical properties were investigated by means of Raman spectra, differential scanning calorimetry (DSC), X-ray diffractometry (XRD) and scanning electron microscopy (SEM). The mechanical strength was measured corresponding to norm ISO 6872. The Raman spectra predominantly showed that small additions of alkaline earth oxides not only form asymmetrical vibrations of the M–Si–O bonds, but also enhance the intensities of symmetrical vibrations of the P–O bonds, making the glass network more stable. And the small additions of CaO or BaO has more influence on the crystallization behaviour, crystalline phase, microstructure and mechanical properties of the glass–ceramics than the addition of MgO. The additions of alkaline earth oxides enhanced the first exothermic peak temperature but decreased the flexural strength of lithium disilicate glass–ceramics.**

**Keywords. Alkaline earth; glass–ceramics; flexural strength; lithium disilicate.**

## 1. Introduction

Glass–ceramics are produced by melting glass and converting it into a unique microstructure by controlled crystallization (McMillan 1982). Microstructure and properties of glass–ceramics were considered to be closely related to the crystallization process (Cheng 1986; Holand *et al* 2003). Headley and Loehman (1986) achieved the volume crystallization in a $SiO_2$–$Li_2O$–$Al_2O_3$–$K_2O$–$B_2O_3$ base glass by small additions of $P_2O_5$ and concluded that the nucleation of lithium metasilicate was catalyzed by the mechanism of heterogeneous nucleation with the principle of epitaxy. Lithium disilicate has been widely used for adherence of ceramics to metals due to its stability below polymorphism temperature and beneficial strength at room temperature (Lin *et al* 2006). As material for dental restorative applications, high mechanical strength is only one of the prerequisites, in order to withstand the masticatory force (Holand *et al* 2006, 2007). Besides mechanical property, the translucent characteristic of glass–ceramics is another important factor that needs consideration (Heffernan *et al* 2002). And Luo and Lu (2009) have investigated the effects of rare-earth oxides ($La_2O_3$ and $Y_2O_3$) on the crystallization behaviour and mechanical properties in the $SiO_2$–$Li_2O$–$Al_2O_3$–$K_2O$–$B_2O_3$ base glass (Luo *et al* 2009), Sun and co-workers (2009) investigated effects of MO (M = Ba, Mg, Ca) on the crystallization of $B_2O_3$–$Al_2O_3$–$SiO_2$ glass–ceramics, and they have gained some favourable results.

In this paper, effects of alkaline earth oxides MO (M = Ba, Mg, Ca) as network modifiers on the structure of glass network, crystallization behaviour and flexural strength of $Li_2O$–$K_2O$–$Al_2O_3$–$Y_2O_3$–$La_2O_3$–$SiO_2$ system glasses were studied. The glass network structure and properties of the glass–ceramics were tested and analysed.

## 2. Experimental

### 2.1 *Glass preparation*

Four glasses in the $Li_2O$–$K_2O$–$Al_2O_3$–$Y_2O_3$–$La_2O_3$–$SiO_2$ system were melted, the chemical composition of all materials used is presented in table 1. Laboratory reagent-grade $Li_2CO_3$, $SiO_2$, $Al_2O_3$, $K_2CO_3$, $BaCO_3$, $CaCO_3$, MgO, $(NH_4)_2HPO_4$ and 5N grade $La_2O_3$, $Y_2O_3$ powders were chosen as the raw materials. These were placed in a quartz crucible which was introduced into a preheated furnace at 450°C to allow for removal of $H_2O$, $CO_2$ and $NH_3$ followed by melting at 1500°C for 2 h. Upon removal of the crucible from the furnace, melted glass was then poured into a pre-heated graphite mould at

*Author for correspondence (axlu@mail.csu.edu.cn)

**Table 1.** Composition of base glasses.

| Samples | Composition (mol%) | | | | | | | | | |
|---|---|---|---|---|---|---|---|---|---|---|
| | $SiO_2$ | $K_2O$ | $Li_2O$ | $Al_2O_3$ | $P_2O_5$ | $Y_2O_3$ | $La_2O_3$ | MgO | CaO | BaO |
| JT0 | 62·00 | 1·20 | 30·80 | 1·50 | 2·50 | 1·20 | 0·80 | – | – | – |
| JT1 | 60·78 | 1·18 | 30·20 | 1·47 | 2·45 | 1·18 | 0·78 | 1·96 | – | – |
| JT2 | 60·78 | 1·18 | 30·20 | 1·47 | 2·45 | 1·18 | 0·78 | – | 1·96 | – |
| JT3 | 60·78 | 1·18 | 30·20 | 1·47 | 2·45 | 1·18 | 0·78 | – | – | 1·96 |

**Table 2.** Heat treatment schedules and precipitated crystalline phases of four glass samples.

| Samples | Heat treatment cycle | Main crystalline | Minor crystallines |
|---|---|---|---|
| JT0 | 520°C/1 h + 615°C/1 h + 750°C/2 h | $Li_2Si_2O_5$ | Quartz, $Li_3PO_4$, cristobalite |
| JT1 | 520°C/1 h + 615°C/1 h + 725°C/2 h | $Li_2Si_2O_5$ | Quartz, $Li_3PO_4$, cristobalite |
| JT2 | 520°C/1 h + 630°C/1 h + 700°C/2 h | $Li_2Si_2O_5$ | Quartz, cristobalite |
| JT3 | 520°C/1 h + 630°C/1 h + 725°C/2 h | $Li_2Si_2O_5$ | Cristobalite |

500°C for 2 h to relieve internal stress. The mould was then allowed to cool to room temperature in the furnace overnight.

### 2.2 *Raman spectra*

The Raman spectra were recorded on a Horiba Jobin Yvon LabRAM HR-800 spectrometer using a He–Ne laser (488 nm) and 8 mW of power before the entrance optics. The measurements were performed on bulk samples and made in the range 200–1500 $cm^{-1}$ at room temperature.

### 2.3 *Differential scanning calorimetry and heat treatment of glasses*

A part of each glass was ground to fine powder for differential scanning calorimetry. Differential thermal analysis (model Netzsch 404 PC) of 50 mg powder of the glass was performed in a dry nitrogen atmosphere at a heating rate of 10°C/min from room temperature to 1000°C. Heat treated schedule for each glass was designed according to DSC results (table 2).

### 2.4 *X-ray diffraction*

After respective heat treatment, the crystalline phases of final glass–ceramics were characterized by XRD. Voltage and current were selected as 40 kV and 50 mA, respectively. Data were collected from $2\theta = 10$–$80°$ at a scanning rate of 10°C/min.

### 2.5 *Scanning electron microscopy*

Highly polished surface of glass–ceramic specimen was etched with 5 vol.% hydrofluoric acid solution for 30 s. After ultrasonic cleaning, specimens were gold sputtered and the microstructure was observed using SEM (FEI Sirion 200).

### 2.6 *Measurement of flexural strength*

Following the instruction of ISO 6872 standard established for strength test of dental ceramics, the three-point bending strength of the bar samples ($4 \times 1{\cdot}2 \times 25$mm with an accuracy $\pm$ 0·02 mm) was measured by using an electronic multipurpose tester (CSS-44100 model, Changchun, China) with a span of 25 mm. Surfaces were ground on wet 320, 400, 600, 800, 1000 grit silicon carbide papers sequentially to produce a flat surface. Five measurements were made on each sample and averaged.

## 3. Results and discussion

### 3.1 *Thermal and structural analysis*

The Raman spectra for this series of glasses are shown in figure 1. The band assignments for all glasses are not characteristic for silicate structure. The most prominent bands at ~ 1070 and ~ 955 $cm^{-1}$ related to the stretching motion of the non-bridging $\nu_s(PO_2)$ in $Q^1$ structure and the in-plane Si–O stretching vibration, respectively (Gopal *et al* 2004; Mogu-Milanković *et al* 2010). And the Raman bands at ~ 590 $cm^{-1}$ belong to symmetrical valence vibrations, $\nu_s$(Si–O–Si group) (Lazarev and Tenisheva 1964). But in the glass specimens JT1, JT2 and JT3 (additions of alkaline-earth oxides), two other bands at ~ 790 and 440 $cm^{-1}$ also appear as major contributors to the Raman spectra, that are assigned to the symmetrical vibrations of the Si–O bonds and the vibrations of the Si–O–Si group of interconnected corner-sharing [$SiO_4$] tetrahedral, respectively (Lazarev and Tenisheva 1964;

Hagiwara and Oyamada 1976). In authors' opinion, the bands at ~785, 783 and 793 $cm^{-1}$ are assigned to the asymmetrical vibrations of the M–Si–O bonds (M = Mg, Ca and Ba), since the sample JT0 with no alkaline earth oxides has no evident band vibrations. Therefore, we should realize that the introduction of alkaline earth oxides interrupts the symmetrical vibrations of the O–Si–O bonds to form the asymmetrical vibrations of M–Si–O bonds. As a result, the intensities of symmetrical vibrations of the P–O bonds at 1070 $cm^{-1}$ increase.

The effects of different alkaline earth oxides on the thermal performance are presented in figure 2. The curves exhibit endothermic peaks due to the glass transition temperature, in the range between 500 and 550°C. All the DSC curves of glass samples are similar to each other, in which there have been two crystallization peaks, one in ~620°C (the first crystallization peak) and the other in ~720°C (second crystallization peak), indicating that all these glass samples have a relative strong tendency to crystallization. By these exothermic peaks temperature we can see that, in these samples doped alkaline earth oxides, the first crystallization peak temperature has increased while the second crystallization peak temperature decreased. The glass samples JT2 and JT3 (introducing CaO and BaO, respectively) have the greatest impact on the crystallization peak temperature (in the specimen JT3, the first crystallization peak temperature increases by 20·9°C and the second crystallization peak temperature decreases by 39·8°C), while the samples introducing MgO have the smallest impact on the crystallization peak temperature. By comprehensive analysis of Raman spectrum data and DSC data, it can be concluded that MO (M = Mg, Ca and Ba) can improve the glass formation of $Li_2O$–$K_2O$–$Al_2O_3$–$Y_2O_3$–$La_2O_3$–$SiO_2$ system. Additive alkaline earth oxides not only form the asymmetrical vibrations of the M–Si–O bonds, but also enhance the intensities of symmetrical vibrations of the P–O bonds, making the glass network more stable in order that the first crystallization peak moves to higher temperature.

In the present study (Fuss *et al* 2006; Kuchler *et al* 2007; Zheng *et al* 2007, 2008), XRD results revealed that lithium metasilicate represented the main crystalline phase after the first crystallization temperature. After further holding at the second crystallization temperature, metastable crystals gave way to lithium disilicate crystals which represented the main crystalline phase of four glass–ceramics after the second crystallization step. In this investigation, to obtain more lithium disilicate crystals, a strict heat-treated route is needed (table 2).

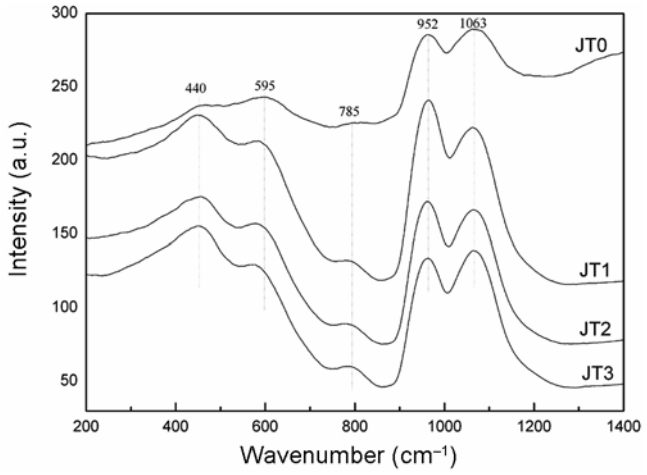


**Figure 1.** Raman spectra of glass specimens.

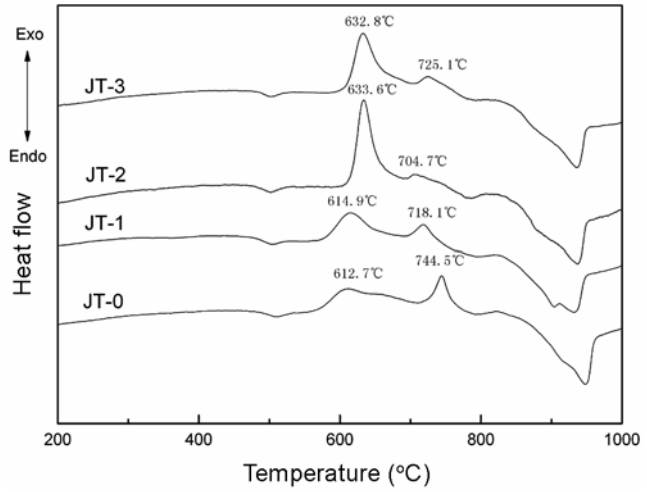


**Figure 2.** DSC results of glass specimens.

## 3.2 *Precipitated crystalline phases*

The general DSC scans of the four glasses in combination with XRD results showed that the crystallization

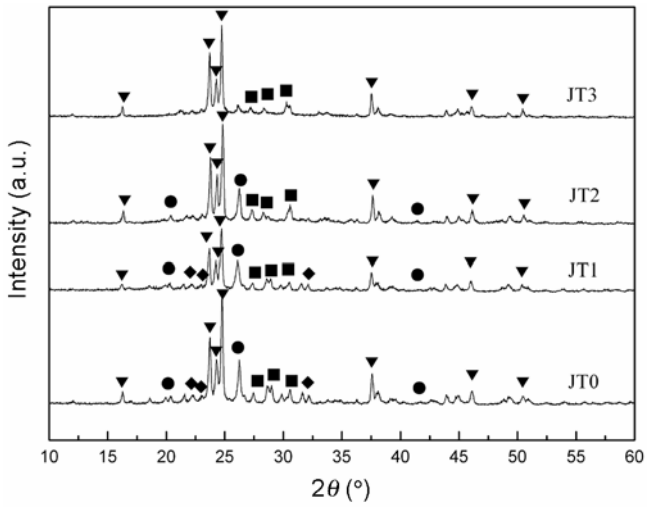


**Figure 3.** XRD patterns of four glass–ceramics: (▼) lithium disilicate; (●) quarz; (□) $Li_3PO_4$ and (■) cristobalite.

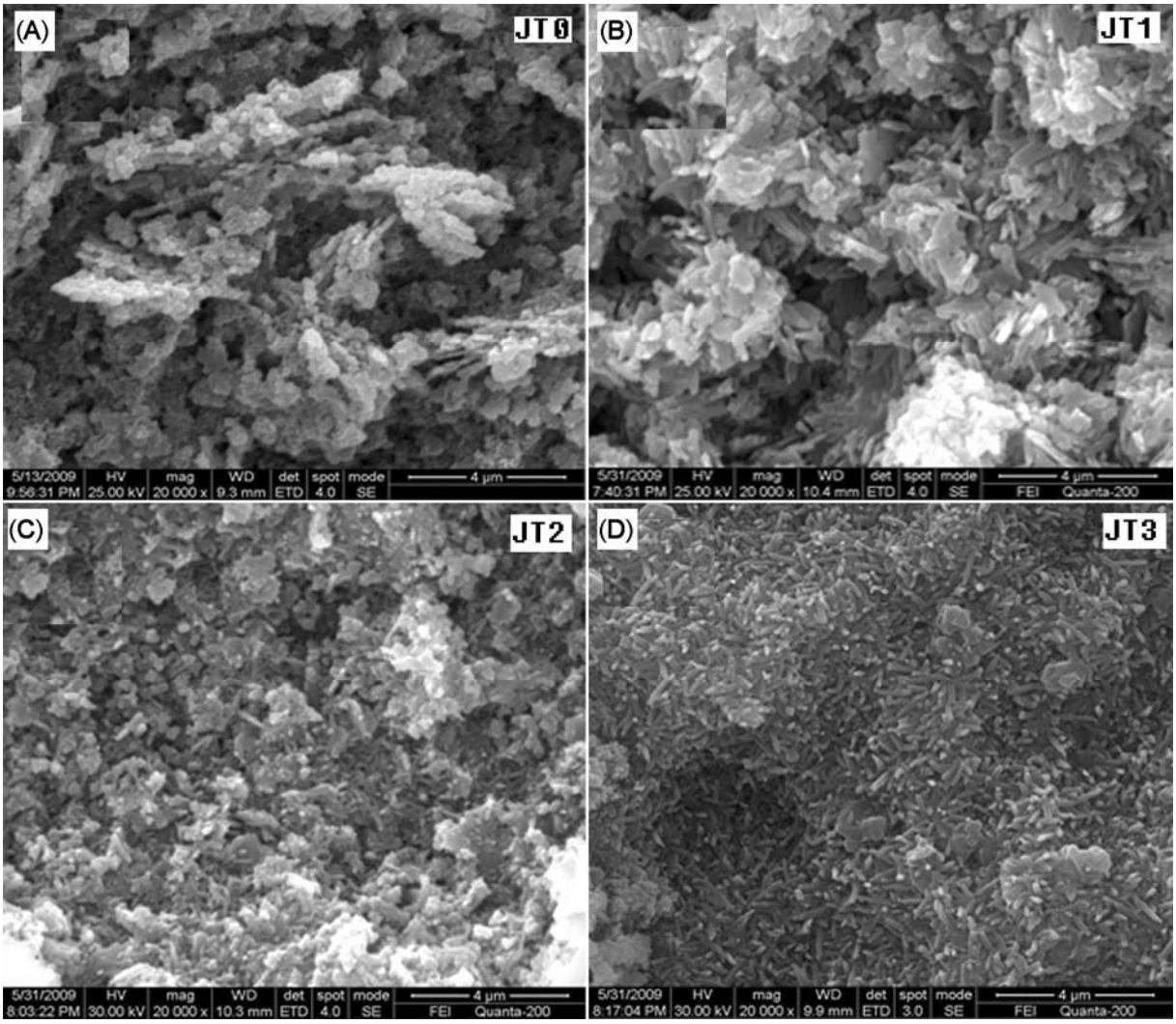


**Figure 4.** SEM photographs of glass–ceramic samples: (**A**) JT0; (**B**) JT1; (**C**) JT2 and (**D**) JT3.

processes of several phases overlapped in glasses. Figure 3 and table 2 show that all the glass–ceramic samples are precipitated in the same main crystalline phase of lithium disilicate, but their second crystalline phase is different. The second crystalline phases of both samples JT1 and JT0 are the quartz, lithium phosphate and cristobalite. But the sample JT1 has higher intensity of the second crystalline phase XRD-peak. Therefore, additive MgO has less effect on crystallization. The second crystalline phases are the quartz and cristobalite for sample JT2 but only the cristobalite for sample JT3, respectively. Samples JT2 and JT3 (additive CaO or BaO) promote the precipitation of crystalline phase of lithium metasilicate but hinder lithium disilicate phase precipitation. From the XRD patterns, there is no residual lithium phosphate crystals in the samples JT2 and JT3. So it is likely that the additive of CaO or BaO obstructs lithium phosphate formation at the stage of nucleation, accordingly it hinders the precipitation of crystal of lithium disilicate and lithium metasilicate crystal transforming to lithium disilicate crystals at the stage of crystallization.

The additive of MgO has less influence on the nucleation of lithium phosphate thus it has little influence on the precipitation of crystals of lithium disilicate. In general, additive of alkaline earth oxides is bad for the precipitation of crystal of lithium disilicate and lithium metasilicate crystal transforming to lithium disilicate crystals. MgO hardly affects the nucleation of lithium phosphate and crystallization of lithium disilicate crystal phase, while the CaO or BaO have great impact on the crystallization of glass from the inhibitory effect.

### 3.3 *Microstructure and flexural strength*

After heat treatment at the heat-treated route (table 2), all glass–ceramic samples were semitransparent. Figure 4 (A)–(D) show scanning electron microscopic photographs of the four samples. The microstructures of the series

reveal that there are areas of varying morphology. The morphology of lithium disilicate crystals in the volume of glass–ceramic samples JT0 and JT1 was lath-shaped and the crystals measured ~ 100 nm–1 mm in length and less than 0·1 nm in width. And the crystals of sample JT0 were more uniform than JT1. The quantity of precipitated lithium disilicate phases in samples JT2 is relatively lesser, whose crystals are close to the irregular shape of hexahedral with smaller aspect ratio than samples JT0 and JT1. The size of crystals in samples JT3 is relatively small (< 1 mm), with fine microstructures of interlocking lithium disilicate crystals in a glassy matrix phase.

The flexural strengths of the glass–ceramics are shown in figure 5. It can be seen that glass–ceramic samples with additive alkaline earth oxides have decreased the value of flexural strength. The value of sample JT1 decreases by 3·36%, which has little effect on the flexural strength. The values of samples JT2 and JT3 decrease by 27·3% and 21·7%, respectively. From SEM photographs, crystal size and crystal shape of samples JT1 and JT0, are relatively similar to each other, respectively. So the flexural strength of the two samples are similar to each other. The sample JT2 with irregular crystal shape, the messy distribution and low crystallization rate have low flexural strength. Although the sample JT3 is of regular crystal shape, uniform crystal distribution, due to small crystal size and low crystallization rate, its flexural strength is still much lower.

Brodkin *et al* (2004) argue that the best properties are obtained when the $Li_2SiO_3$ and silica phases are nearly absent, the volume fraction of $Li_3PO_4$ is less than about 5% and the volume fraction of $Li_2Si_2O_5$ is between about 35–60%. High aspect ratio morphology of $Li_2Si_2O_5$ phase is important to enhance flexural strength of the glass–ceramics. In this study, all of the glass–ceramic samples are with the main phase of lithium disilicate, free of lithium metasilicate and less of $Li_3PO_4$. The lithium disilicate crystals of samples JT0 and JT1 have high aspect ratio (from 2 to 10), of whom the flexural strength was significantly higher than JT2 and JT3.

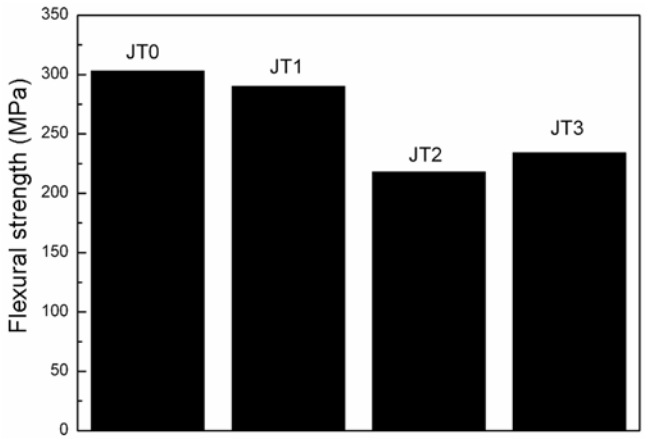


**Figure 5.** Flexural strength of four glass–ceramics.

## 4. Conclusions

In this study, glass network structure, crystallization behaviour and flexural strength of lithium disilicate glass–ceramics in the $Li_2O$–$K_2O$–$Al_2O_3$–$Y_2O_3$–$La_2O_3$–$SiO_2$ system with additive alkaline earth oxides were analysed. The interrelations between different additive alkaline earth, microstructure and flexural strength were discussed. The outcome of this research can be summarized as follows:

(I) MO (M = Mg, Ca and Ba) can improve the glass formation of $Li_2O$–$K_2O$–$Al_2O_3$–$Y_2O_3$–$La_2O_3$–$SiO_2$ system. Additive alkaline earth oxides not only formed the asymmetrical vibrations of the M–Si–O bonds, but also enhanced the intensities of symmetrical vibrations of the P–O bonds, making the glass network more stable in order that the first crystallization peak moves to higher temperature.

(II) Additive of alkaline earth oxides was bad for the precipitation of crystal of lithium disilicate and lithium metasilicate crystal transforming to lithium disilicate crystals. MgO hardly affects the nucleation of lithium phosphate and crystallization of lithium disilicate crystal phase, while CaO or BaO have great impact on the crystallization of glass from the inhibitory effect.

(III) All glass–ceramic samples were semi-transparent after heat treatment. Additive of alkaline earth oxides decreased the flexural strength of lithium disilicate glass–ceramics.

## Acknowledgement

The research was financially supported by the Key Materials Research Foundation of P.R. China (No. JPPT-115-332).

## References

Brodkin D, Orange W, Panzera C, Mead B, Panzera P and Holly M 2004 U.S. patent 6,802,894

Cheng J J J 1986 *Non-Cryst. Solids* **80** 52

Fuss T, Ray C S, Lesher C E and Day D E 2006 *J. Non-Cryst. Solids* **352** 2073

Gopal N O, Narasimhulu K V and Rao J L 2004 *Spectrochimica Acta* **A60** 2441

Hagiwara H and Oyamada R 1976 *J. Phys. Soc. Jpn.* **40** 199

Headley J and Loehman R E 1986 *J. Am. Ceram. Soc.* **67** 620

Heffernan M J, Aquilino S A, Diaz-Arnold A M, Haselton D R, Stanford C M and Vargas M A 2002 *J. Prosthet. Dent.* **88** 4

Holand W, Rheinberger V and Schweiger M 2003 *Philos. Trans. R. Soc. London* **A361** 575

Holand W, Rheinberger V, Apel E and Van't H C 2007 *J. Eur. Ceram. Soc.* **27** 1521

Holand W, Rheinberger V, Apel E, Van't H C, Holand M, Dommann A, Obrecht M, Mauth C and Graf-Hausner U 2006 *J. Mater. Sci.: Mater. Med.* **17** 1037

Kuchler R, Kanert O, Vereget T and Jain H 2007 *J. Non-Cryst. Solids* **353** 3940

Lazarev A N and Tenisheva T F 1964 *J. Str. Chem.* **4** 647

Lin C C, Shen P, Chang H M and Yang Y J 2006 *J. Eur. Ceram. Soc.* **26** 3613

Luo Z W and Lu A X 2009 *Chinese J. Nonferrous Metals* **19** 1264

Luo Z W, Lu A X and Han L G 2009 *Chinese J. Nonferrous Metals* **19** 2018

McMillan P W 1982 *J. Non-Cryst. Solids* **52** 67

Mogu-Milanković A, Pavić L, Reis S T, Day D E and Ivanda M 2010 *J. Non-Cryst. Solids* **356** 715

Sun T, Xiao H N, Cheng Y and Liu H 2009 *Ceram. Int.* **35** 1051

Zheng X, Wen G W and Song L 2007 *Acta Mater.* **55** 3583

Zheng X, Wen G W, Song L and Huang X X 2008 *Acta Mater.* **56** 549